



Radiation defects and intrinsic luminescence of cancrinite

Ekaterina Kaneva^{a,b}, Roman Shendrik^{a,*}

^a Vinogradov Institute of Geochemistry SB RAS, 1a Favorskogo Str., Irkutsk, 664 033, Russia

^b Department of Subsoil Use, Irkutsk National Research Technical University, 664 074, Irkutsk, Russia

ARTICLE INFO

Keywords:

Carbonate radical
Microporous
Intrinsic luminescence
Radiation defects
Cancrinite

ABSTRACT

The study of hole radiation defects and intrinsic luminescence in microporous cancrinite is carried out. It is shown that nonradiative decay of electronic excitations at temperatures above 120 K leads to the formation of hole radicals $(\text{CO}_3)^{\cdot-}$. The intrinsic luminescence of cancrinite is attributed to the radiative recombination of electronic excitations.

1. Introduction

A cancrinite is an aluminosilicate belonging to the feldspathoid mineral family. The crystal structure of the compound (Fig. 1) is characterized by layers of the six-membered ring of Si- and Al-centered tetrahedra, which form a three-dimensional framework. The rings surround the cancrinite-type (CAN) cavities and structural channels. Cancrinite contains carbonate and chlorine anions in the voids of the channels. Sodium and calcium ions also occupy the in-channel positions around the carbon-centered triangles. Sodium atoms and water molecules are alternately located in the center of the CAN cavities.

Materials with a cancrinite structure were proposed for the storage of liquid radioactive waste [1]. Cancrinite-type materials show promising photocatalytic properties [2,3]. They could be a perspective host for polymers isolated in a dielectric matrix [4], oriented fluorescent dyes [5], photochemistry [6–8], solar energy conversion devices [9] and photonic crystals [10], as well as the combined effect of adsorption enthalpy and entropy in the diffusion dynamics of adsorbed molecules [11]. The structural properties and lattice dynamics of microporous natural and synthetic compounds of the cancrinite group have been intensively studied [12]. We have found that ultraviolet (UV) irradiation creates carbonate radicals in cancrinite [13]. That makes it possible to use cancrinite in photochemical water purification systems. However, the mechanism of electronic defect creation under UV, vacuum ultraviolet (VUV), and X-ray excitation are not well investigated.

Most of the studies were focused on the cancrinite materials co-doped with Se. These samples demonstrated a broad photoluminescence band peaked at 1.4 eV under 2.4 eV excitation attributed

to Se_2^- centers. Photoionization of Se_2^{2-} ions under UV irradiation forms Se_2^- centers in the cancrinite channels [14]. Organic molecules and lanthanides ions in cancrinite cages showed photoluminescence in other zeolite-like materials [15,16]. An intrinsic luminescence peaked at 3.6 eV was found in other stressed microporous silicates [17,18].

The intrinsic luminescence and radiation defect formation mechanisms in microporous materials have been studied during the past 50 years. The detailed investigation was focused on sodalite ceramics containing halogen ions [20–27], and sulfoaluminates [28].

Sodalite materials containing Cl ions in sodalite cages demonstrate intrinsic luminescence in 2–4.5 eV spectral region under 6 eV excitation. Luminescence peaked at 2.5–3.7 eV was observed in Br-sodalites [20, 25]. Three luminescence bands with maxima at 2.8, 3.6, and 4.2 eV were found in I-sodalite [21]. Observed luminescence peaked at 3.6 eV is attributed to radiative decay of electronic excitations near Na_3I defect cages. 4.2 eV emission band corresponds to decay of electronic excitations near Na_4I cages. Imperfect cages (Br^- and/or Na^+ is absent) actively participate in the process of luminescence excitation and the creation of F centers in Br sodalites under VUV excitation [22]. Intrinsic luminescence is not studied in cancrinite. In the present work, we investigate the intrinsic luminescence and electronic defect formation processes in cancrinite under UV/VUV and X-ray excitations.

2. Methodology

The samples were extracted from the nepheline syenites at the Zhidoi alkaline complex (Tunka Range, Siberian Craton, Russia). Cancrinite occurs as aggregates of coarse prismatic grains. Samples range in color

* Corresponding author.

E-mail address: r.shendrik@gmail.com (R. Shendrik).

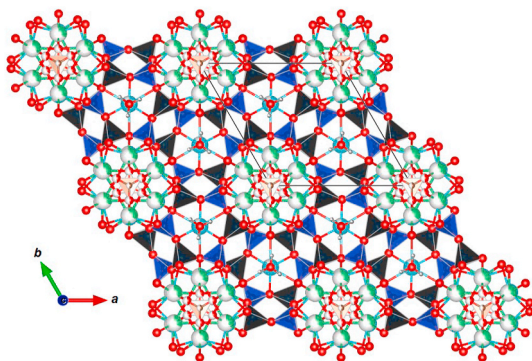


Fig. 1. Crystal structure of the studied cancrinite projected along the *c* axis. Si and Al-centered tetrahedra are blue and black, respectively. Oxygen atoms are drawn in red. Na and Ca atoms are cyan and light green, respectively. C atoms are brown and H atoms (hydrogens of H₂O molecule) are drawn in grey. The partially white coloring of the spheres indicates a vacancy. The figure was prepared in the program VESTA (version 4.3.0) [19] using single-crystal data obtained in Ref. [13].

from brownish pink to grayish pink and are translucent to opaque. Under a binocular microscope, the cancrinite grains were carefully handpicked and cleaned off contaminants, mainly aegirine and nepheline. The part of samples was powdered to 0.02 mm and then was verified using the X-ray powder diffractometer D8 ADVANCE (Bruker). The analysis of the chemical composition and crystal structure of studied cancrinite has been performed [13].

The established crystal-chemical formula, calculated on the basis of 12(Si + Al) per formula unit, for the investigated cancrinite is Na_{6.47}Ca_{1.23}K_{0.01} [Al_{5.97}Si_{6.03}O₂₄](CO₃)_{1.45}(SO₄)_{0.03}Cl_{0.01} · 2H₂O [13]. Cancrinite has a hexagonal unit cell (Fig. 1). Two mutually exclusive configurations of the CO₃ anionic group occupy the center of the channels in the crystal structure of the studied cancrinite. A characteristic feature of the samples under study is the disordering of the cationic position into two sub-positions. In addition, in our samples, the Ow position (oxygen of the H₂O molecule) is situated on the threefold axis, which is rare since Ow displacement from the ideal position at (2/3, 1/3, z) was observed in most of the previously published structural models. The revealed features of the crystal structure of studied cancrinite [13] are unique since they have not previously been found in such a combination among the structural characteristics of cancrinite samples from other deposits.

Photoluminescence spectra were recorded using an MDR-2 monochromator with a grating having 1200 lines per mm and a Hamamatsu photomodule operating in the photon counting mode. Excitation was carried out using a Hamamatsu L7293-50 deuterium lamp with a magnesium fluoride window through a VMR-2 vacuum monochromator. The excitation spectra were corrected using sodium salicylate. The sample was attached to the cryofinger using a thermal silver paste, which does not emit under the VUV excitation, and placed in a pumped closed-cycle cryostat.

Electron spin resonance (ESR) spectra were recorded using a RE-1306 X-band spectrometer with a frequency of 9.257 GHz. A single crystal was placed in a test tube. The measurements were carried out at room temperature and in a quartz cryostat at 77 K.

The crystals were irradiated using an X-ray tube with a Pd anode driven by 40 kV at 20 mA for 10 min at room temperature. Optical absorption spectra of the samples were measured on a PerkinElmer Lambda 950 spectrophotometer in the integrating sphere at room temperature [29].

The following procedure is used to measure a thermal bleaching curve. The sample was heated with step 50 K and kept at this temperature for 5 min. Then it was cooled down to room temperature, and the ESR and optical absorption spectra were measured again until the

absorption and the ESR signal disappeared.

The measurement of a spectrum of creation of (CO₃)⁻ radical was performed by the following procedure. The sample was irradiated for 30 min using a Hamamatsu L7293-50 deuterium lamp with a magnesium fluoride window through a VMR-2 vacuum monochromator. Next, the ESR signal from the induced centers was measured at room temperature. After that, the sample was thermally bleached at 573 K and irradiated with the next wavelength.

The following technique was used to measure the temperature dependence of the creation of radiation defects in cancrinite crystals. The sample was placed in a dewar with liquid nitrogen vapor and irradiated by a low-pressure mercury lamp ($\lambda = 198$ nm) for 10 min. The temperature was monitored using a type-K thermocouple. After irradiation, the sample was placed in a cryostat at 77 K, and the ESR spectrum of induced radiation defects was measured. This procedure was repeated at temperatures ranging from 80 to 235 K.

The absorption and ESR spectra of the sample irradiated with a low-pressure mercury lamp coincide with the spectra of the X-irradiated sample.

3. Results

The studied samples of cancrinite contain a small number of impurity centers. Therefore, impurity luminescence is not detected. However, an intrinsic luminescence is observed at low temperatures under excitation in the region of fundamental absorption. The spectrum is shown in Fig. 2. Two broad bands with maxima at 3.8 and 2.8 eV are observed. The excitation spectra monitored in both bands coincide. The excitation spectrum consists of a rise at 5.4 eV, a slight dip at 5.6 eV, and an intensive peak at 6.2 eV. The luminescence is quenched at the heating of the sample above 220 K. The temperature dependence of the luminescence intensity is shown in Fig. 3.

The cancrinite acquires a blue color under irradiation at room temperature. In the absorption spectrum of the irradiated crystal, an intense band with a maximum at 2 eV is observed (Fig. 4). This absorption is attributed to (CO₃)⁻ radicals [13]. Also, an ESR signal attributed to this centers with $g_y = 2.014$ and $g_x = 2.018$ appears in the irradiated samples (Fig. 5). Fig. 2 (blue dots) shows the dependence of the number of created (CO₃)⁻ radicals on the irradiation energy. The number of the radicals was estimated from the integral intensity of the ESR signal. The figure shows that the radicals are created after irradiation with energies above 6 eV.

The efficiency of radiation coloration of the sample during cooling decreases significantly. It is no longer staining at temperatures below 120 K (Fig. 3). At the same time, the intensity of the intrinsic luminescence increases with cooling.

The cancrinite irradiated at room temperature becomes discolored during heating above 500 K. The ESR signal is not registered in the bleached sample. The temperature dependencies of the destruction of

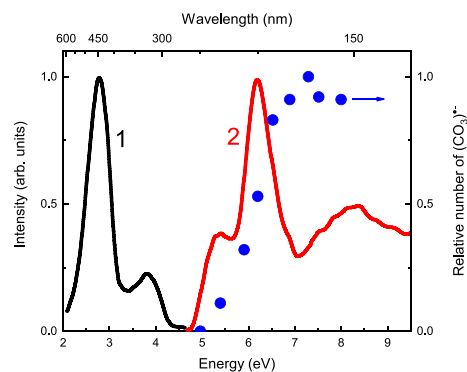


Fig. 2. Luminescence spectra (curve 1) at 6 eV excitation (curve 2), measured at 80 K. The blue dots show the creation efficiency of (CO₃)⁻ radical at 300 K.

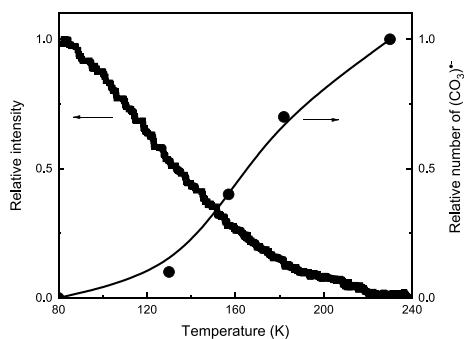


Fig. 3. Temperature dependence of luminescence monitored at 2.8 eV (squares) and efficiency of $(\text{CO}_3)^{\bullet-}$ radical creation (circles) under 198 nm irradiation.

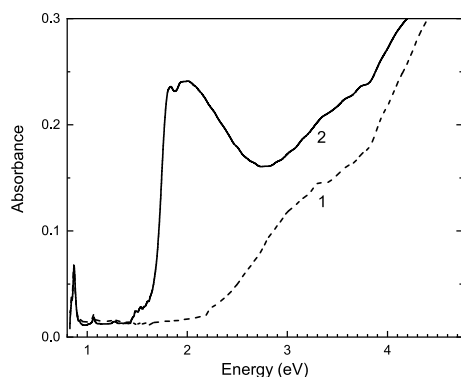


Fig. 4. Absorption spectra of cancrinite before (curve 1) and after (curve 2) irradiation.

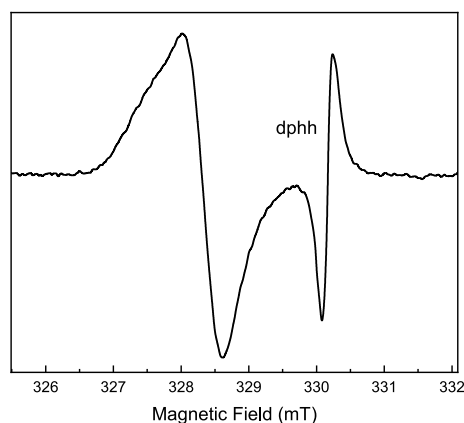


Fig. 5. ESR spectrum of irradiated cancrinite.

the $(\text{CO}_3)^{\bullet-}$ radicals in cancrinite calculated from the absorption and ESR spectra are shown in Fig. 6. The activation energy of this process is estimated using the Garlick-Gibson kinetics of the second order for the thermally stimulated process [30]. The activation energy is about 0.91 eV with a frequency factor 10^8 Hz. Thermally stimulated luminescence is not observed during the heating of cancrinite.

4. Discussion

In the X-irradiated samples the absorption band at 2 eV and the ESR signal appear. They correspond to the $(\text{CO}_3)^{\bullet-}$ radicals [13]. Similar absorption and ESR were observed in neutron and X-irradiated calcite (CaCO_3) [31], potassium bicarbonate (KHCO_3) [32], naturally

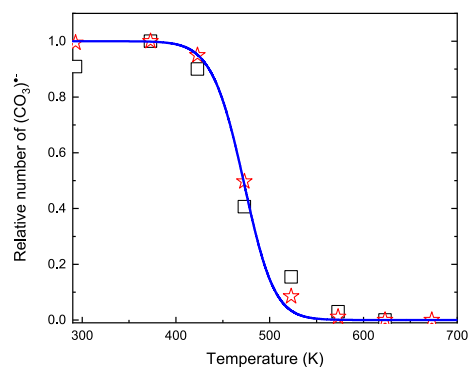


Fig. 6. Temperature stability of ESR (stars) and optical absorption (squares) bands attributed to $(\text{CO}_3)^{\bullet-}$ centers in cancrinite.

irradiated Maxixe beryl ($\text{Be}_3\text{Al}_2(\text{Si}_6\text{O}_{18})$) containing CO_3^{2-} anions in channels [33].

The $(\text{CO}_3)^{\bullet-}$ radicals are induced in cancrinite under X-ray or UV irradiation (Figs. 2 and 5). This fact indicates that the excitation of carbonate complexes $(\text{CO}_3)^{2-}$ occurs. In calcite, the fundamental absorption edge was observed in 6 eV spectral region. The top of the valence band is produced by mixing of C and O 2p and 2s states within the carbonate group [34]. The highest states demonstrate a significant O 2s character with some mixing of Ca 3p states, that facilitate charge transfer from 4s orbital states to anionic C and O orbitals [35]. Therefore, we can conclude that transition within the carbonate group is located in cancrinite in the region of 6 eV, similarly to that observed in calcite. Upon excitation in this region, the carbonate complex ionizes with the formation of the $(\text{CO}_3)^{\bullet-}$ radical.

At the same time, the absorption increases in 2.8–4 eV region. The absorption of electronic F and F^+ centers in calcium oxide lies in this region. F and F^+ centers represent anionic oxygen vacancies, capturing two or one electrons [36]. On the other hand, the excitonic mechanism of defect creation cannot occur in simple oxides because displacement energies for both anion and cation species are significantly larger than 6 eV [37]. In zeolites the displacement energies of oxygen anions and cations are about 40–60 eV and 20 eV, respectively [38]. Therefore, vacancies cannot be created under 6 eV irradiation.

As pointed above, the $\text{CO}_3^{\bullet-}$ radicals are not formed in calcite, beryl, and other carbonate-containing materials under UV or VUV radiation, because of energy of UV/VUV photons is not enough to create electron capture centers, that could be acceptors for electrons from ionized CO_3 . Thus, the formation of stable $\text{CO}_3^{\bullet-}$ radicals requires the creation of electron traps paired with them. The carbonate radicals are created in NaHCO_3 and Na_2CO_3 solutions under UV irradiation due to the reaction between bi/carbonate ions and HO^{\bullet} . Where HO^{\bullet} radical is also induced under UV radiation [39].

The channels of cancrinite contain $(\text{CO}_3)^{2-}$ and Cl^- anions, lying in two mutually exclusive and partially occupied positions in the center of the channel, and cation site, distributed into two split positions of sodium and calcium [13]. Partially occupied positions mean that anionic and cationic vacancies are located in the channels. The anionic vacancy can trap an electron after bicarbonate anion ionization. In Ref. [22] it was found that the irradiation of nonstoichiometric sodalites containing anionic vacancies causes an efficient creation of F-centers. Therefore, F-like centers attributed to anionic vacancies in the channels can be electronic defects created due to nonradiative decay of electronic excitations in cancrinite. The absorption rise in the region 2.8–4 eV could be attributed to this type of electronic defect. However, the origin of electron traps in cancrinite should still be clarified.

The intrinsic luminescence was registered for the first time in cancrinite. In Ref. [20] luminescence in the region of 2–3 eV corresponds to the decay of electronic excitations of aluminosilicate cage. Luminescence band in quartz in the 2.7 eV region is associated with self-trapped

excitons [40]. Luminescence bands in sodalite-like materials are located in the 2.8–4.2 eV range. They were attributed to radiative decay of electronic excitations in sodalite cages [21,22].

The observed excitation spectrum (Fig. 2) is typical for intrinsic luminescence in oxides [23,40–43]. The dip in the excitation spectrum in the region of 5.6 eV is associated with the presence of a fundamental absorption peak attributed to transitions from 2p O states to mixed C and O 2p and 2s and Ca 3d states. Thus, we can estimate the energy of the bandgap of cancrinite according to the VRBE method [44–46]. The bandgap is about 6.1 eV.

As shown in Fig. 3, the efficiency of $(\text{CO}_3)^{\cdot-}$ radical production decreases during cooling. At the same time, the intensity of intrinsic luminescence increases (Fig. 3) with cooling. This anticorrelation behavior is similar to observed before in alkali-halides [47], alkali-earth halides [48–50] and oxides [27,51]. This fact is evidence that an excitonic mechanism of defect creation takes place.

The photoionization of the 2s shell of oxygen ions causes the formation of electron-holes e–h pairs with the participation of 2s and 2p oxygen shells [52,53]. As a result, electronic excitations are formed. Their decay provides especially favorable conditions for the creation of temperature-stable $(\text{CO}_3)^{\cdot-}$ hole centers. They become stable up to 500 K (Fig. 6). At higher temperatures, destruction of $(\text{CO}_3)^{\cdot-}$ centers occurs with nonradiative recombination. The destruction of carbonate radicals was observed at 440 K in BaCO_3 [54].

5. Conclusion

The intrinsic luminescence in cancrinite crystals was found and studied for the first time. The luminescence observed at temperatures below 150 K with two maxima at 3.8 and 2.8 eV is associated with radiative recombination of electronic excitations near oxygen ions. Hole radicals $(\text{CO}_3)^{\cdot-}$ are formed as a result of the nonradiative decay of electronic excitations at temperatures above 150 K.

Credit author statement

Ekaterina Kaneva: Writing - Review and Editing, Conceptualization, Methodology, Investigation, Resources, Funding acquisition, Supervision. Roman Shendrik: Conceptualization, Methodology, Writing - Original Draft, Writing - Review and Editing, Investigation, Formal Analysis, Validation, Visualization.

Declaration of competing interest

The authors declare that they have no known competing financial interests or personal relationships that could have appeared to influence the work reported in this paper.

Acknowledgments

The authors gratefully acknowledge Tatiana Radomskaya, who kindly provided the cancrinite sample studied in this work. The study was carried out using facilities of the Centers for Collective Use: “Center for isotopic-geochemical investigations” at the Vinogradov Institute of Geochemistry SB RAS.

This research was performed under the project 0284-2021-0004 “Materials and Technologies for the Development of Radiation Detectors, Luminophores, and Optical Glasses”. The structural and luminescence investigations was partially funded by INRTU, grant number 15-RAS-2020 (Grant of the University Council).

References

- [1] E.C. Buck, B.K. McNamara, Precipitation of nitrate- cancrinite in hanford tank sludge, *Environ. Sci. Technol.* 38 (16) (2004) 4432–4438, <https://doi.org/10.1021/es034943i>.
- [2] M. Miyake, T. Akachi, M. Matsuda, Preparation, structure and photocatalytic properties of cancrinite encapsulating lead and sulfide ions, *J. Mater. Chem.* 15 (7) (2005) 791–797, <https://doi.org/10.1039/B411431K>.
- [3] S. Bahrani, M. Ghaedi, R. Tariq, Z. Zalipour, F. Sadeghfah, Fundamental developments in the zeolite process, in: *Interface Science and Technology* vol. 32, 2021, pp. 499–556, <https://doi.org/10.1016/B978-0-12-818806-4.00003-6>.
- [4] C.O. Areán, Zeolites and intrazeolite chemistry: insights from infrared spectroscopy, *Comments Mod. Chem.* 22 (3–4) (2000) 241–273, <https://doi.org/10.1080/02603590008050871>.
- [5] M. Busby, H. Kerschbaumer, G. Calzaferri, L. De Cola, Orthogonally bifunctional fluorescent zeolite-L microcrystals, *Adv. Mater.* 20 (9) (2008) 1614–1618, <https://doi.org/10.1002/adma.200702354>.
- [6] S. Hashimoto, Zeolite photochemistry: impact of zeolites on photochemistry and feedback from photochemistry to zeolite science, *J. Photochem. Photobiol. C Photochem. Rev.* 4 (1) (2003) 19–49, [https://doi.org/10.1016/S1389-5567\(03\)00003-0](https://doi.org/10.1016/S1389-5567(03)00003-0).
- [7] Y. Li, L. Li, J. Yu, Applications of zeolites in sustainable chemistry, *Inside Chem.* 3 (6) (2017) 928–949, <https://doi.org/10.1016/j.jchempr.2017.10.009>.
- [8] J.A. Moreno-Torres, M. Flores-Acosta, R. Ramírez-Bon, E. Coutino-Gonzalez, Lead confinement and fluorimetric detection using zeolites: towards a rapid and cost-effective detection of lead in water, *J. Phys.: Photonics* 3 (3) (2021), 034003, <https://doi.org/10.1088/2515-7647/abf945>.
- [9] S. Huber, G. Calzaferri, Light-harvesting host-guest antenna materials for solar energy conversion devices, in: *Photonics for Solar Energy Systems*, vol. 6197, 2006, p. 619708, <https://doi.org/10.1117/12.661153>.
- [10] S. Mintova, M. Jaber, V. Valtchev, Nanosized microporous crystals: emerging applications, *Chem. Soc. Rev.* 44 (20) (2015) 7207–7233, <https://doi.org/10.1039/C5CS00210A>.
- [11] M.R. Delgado, A.M. de Yuso, R. Bulánek, C.O. Areán, Infrared spectroscopic and thermodynamic assessment of extraframework cationic adsorption sites in the zeolite KL by using CO as probe molecule, *Chem. Phys. Lett.* 639 (2015) 195–198, <https://doi.org/10.1016/j.cplett.2015.09.028>.
- [12] N. Chukanov, S. Aksenov, R. Rastsvetaeva, Structural chemistry, IR spectroscopy, properties, and genesis of natural and synthetic microporous cancrinite- and sodalite-related materials: a review, *Microporous Mesoporous Mater.* (2021) 111098, <https://doi.org/10.1016/j.micromeso.2021.111098>.
- [13] R. Shendrik, E. Kaneva, T. Radomskaya, I. Sharygin, A. Marfin, Relationships between the structural, vibrational, and optical properties of microporous cancrinite, *Crystals* 11 (3) (2021) 280, <https://doi.org/10.3390/cryst11030280>.
- [14] V.V. Poborchii, G.-G. Lindner, M. Sato, Selenium dimers and linear chains in one-dimensional cancrinite nanochannels: structure, dynamics, and optical properties, *J. Chem. Phys.* 116 (6) (2002) 2609–2617, <https://doi.org/10.1063/1.1434950>.
- [15] L. Chen, B. Yan, Luminescent hybrid materials based on zeolite L crystals and lanthanide complexes: host-guest assembly and ultraviolet-visible excitation, *Spectrochim. Acta Mol. Biomol. Spectrosc.* 131 (2014) 1–8, <https://doi.org/10.1016/j.saa.2014.04.079>.
- [16] L. Chen, B. Yan, Multi-component lanthanide hybrids based on zeolite A/L and zeolite A/L-polymers for tunable luminescence, *Photochem. Photobiol. Sci.* 14 (2) (2015) 358–365, <https://doi.org/10.1039/C4PP00364K>.
- [17] J. Garcia-Guinea, V. Correcher, L. Sanchez-Munoz, A. Finch, D. Hole, P. Townsend, On the luminescence emission band at 340 nm of stressed tectosilicate lattices, *Nucl. Instrum. Methods Phys. Res. Sect. A Accel. Spectrom. Detect. Assoc. Equip.* 580 (1) (2007) 648–651, <https://doi.org/10.1016/j.nima.2007.05.111>.
- [18] V. Fuentes, J. Fernández, E. Enríquez, Enhanced luminescence in rare-earth-free fast-sintering glass-ceramic, *Optica* 6 (5) (2019) 668–679, <https://doi.org/10.1364/OPTICA.6.000668>.
- [19] K. Momma, F. Izumi, VESTA 3 for three-dimensional visualization of crystal, volumetric and morphology data, *J. Appl. Crystallogr.* 44 (6) (2011) 1272–1276, <https://doi.org/10.1107/S0021889811038970>.
- [20] V. Denks, A. Dudel'zak, C.B. Lushchik, T. Ruus, N. Soshchin, T. Trofimova, Recombination luminescence and color centers of cathodochromic sodalites, *J. Appl. Spectrosc.* 24 (1) (1976) 23–28.
- [21] M. Kirm, V. Demidenko, V. Denks, E. Feldbach, A. Lushchik, C. Lushchik, I. Martinson, Excitations in halogen-containing aluminosilicate optical ceramics, *J. Electron. Spectrosc. Relat. Phenom.* 101 (1999) 593–597, [https://doi.org/10.1016/S0368-2048\(98\)00338-7](https://doi.org/10.1016/S0368-2048(98)00338-7).
- [22] C. Lushchik, V. Demidenko, M. Kirm, I. Kudryavtseva, A. Lushchik, I. Martinson, V. Nagirnyi, E. Vasil'chenko, Creation of F centres and multiplication of electronic excitations in $\text{Na}_6\text{Al}_6\text{Si}_6\text{O}_{24}(\text{NaBr})_{2x}$ optical ceramics under VUV irradiation, *J. Phys. Condens. Matter* 13 (27) (2001) 6133, <https://doi.org/10.1088/0953-8984/13/27/307>.
- [23] A. Lushchik, M. Kirm, C. Lushchik, I. Martinson, V. Nagirnyi, E. Vasil'chenko, Nano-scale radiation effects in wide-gap crystals under irradiation by VUV photons, *Nucl. Instrum. Methods Phys. Res. Sect. B Beam Interact. Mater. Atoms* 191 (1–4) (2002) 135–143, [https://doi.org/10.1016/S0168-583X\(02\)00531-1](https://doi.org/10.1016/S0168-583X(02)00531-1).
- [24] A. Lushchik, M. Kirm, I. Kudryavtseva, C. Lushchik, I. Martinson, V. Nagirnyi, E. Vasil'chenko, Creation of electronic excitations and defects by VUV radiation (6–40 eV) in wide-gap solids, *Radiat. Eff. Defect Solid* 157 (6–12) (2002) 537–543, <https://doi.org/10.1080/10420150215747>.
- [25] V. Denks, T. Karner, V. Murk, Electron-hole processes in nonstoichiometric I-and Br-sodalite powders and optical ceramics, in: *Optical Inorganic Dielectric Materials and Devices*, vol. 2967, 1997, pp. 63–68, <https://doi.org/10.1117/12.266509>.
- [26] R. Denisov, V. Denks, A. Dudel'zak, V. Osminin, T. Ruus, Optical destructible coloring and luminescence of sodalites, *J. Appl. Spectrosc.* 27 (1) (1977) 934–938.
- [27] I. Kudryavtseva, P. Liblik, A. Lushchik, C. Lushchik, V. Nagirnyi, E. Vasil'chenko, Color center formation by synchrotron radiation in the $\text{Na}_6\text{Al}_6\text{Si}_6\text{O}_{24}(\text{Na})_{1.6}$

- optical ceramic, *Phys. Solid State* 43 (5) (2001) 830–835, <https://doi.org/10.1134/1.1371360>.
- [28] M.L. Phillips, L.E. Shea, D.R. Tallant, R.J. Walko, T.M. Nenoff, Reduced sulfoaluminate as cathodoluminescent phosphors, in: *Physics and Chemistry of Luminescent Materials: Proceedings of the Eighth International Symposium*, vol. 99, The Electrochemical Society, 2000, p. 45.
- [29] D. Sofich, Y. Tushinova, R. Shendrik, B. Bazarov, S. Dorzhieva, O. Chimitova, J. Bazarova, Optical spectroscopy of molybdates with composition $\text{Ln}_2\text{Zr}_3(\text{MoO}_4)_9$ (Ln: Eu, Tb), *Opt. Mater.* 81 (2018) 71–77, <https://doi.org/10.1016/j.optmat.2018.05.028>.
- [30] G. Garlick, A. Gibson, The electron trap mechanism of luminescence in sulphide and silicate phosphors, *Proc. Phys. Soc.* 60 (6) (1948) 574, <https://doi.org/10.1088/0959-5309/60/6/308>, 1926–1948.
- [31] R. Serway, S. Marshall, Electron spin resonance absorption spectra of textCO_3^- and textCO_3^{ms} molecule—ions in irradiated single-crystal calcite, *J. Chem. Phys.* 46 (5) (1967) 1949–1952, <https://doi.org/10.1063/1.1840958>.
- [32] Z. Top, S. Raziell, Z. Luz, B.L. Silver, ESR of the radical-ion $\text{CO}_3^{\cdot-}$ in gamma-irradiated potassium bicarbonate, *J. Magn. Reson.* 12 (2) (1973) 102–108, [https://doi.org/10.1016/0022-2364\(73\)90132-7](https://doi.org/10.1016/0022-2364(73)90132-7), 1969.
- [33] M. Pinheiro, K. Krambrock, K. Guedes, J.-M. Spaeth, Optically-detected magnetic resonance of molecular color centers CO_3^- and NO_3 in gamma-irradiated beryl, *Phys. Status Solidi C* 4 (3) (2007) 1293–1296, <https://doi.org/10.1002/pssc.200673825>.
- [34] D. Baer, D.L. Blanchard Jr., Studies of the calcite cleavage surface for comparison with calculation, *Appl. Surf. Sci.* 72 (4) (1993) 295–300, [https://doi.org/10.1016/0169-4332\(93\)90365-1](https://doi.org/10.1016/0169-4332(93)90365-1).
- [35] F.M. Hossain, G.E. Murch, I.V. Belova, B.D. Turner, Electronic, optical and bonding properties of CaCO_3 calcite, *Solid State Commun.* 149 (29–30) (2009) 1201–1203, <https://doi.org/10.1016/j.ssc.2009.04.026>.
- [36] B. Henderson, Y. Chen, W. Sibley, Temperature dependence of luminescence of F^+ and F centers in CaO , *Phys. Rev. B* 6 (10) (1972) 4060, <https://doi.org/10.1103/PhysRev.183.826>.
- [37] A. Popov, E. Kotomin, J. Maier, Basic properties of the F-type centers in halides, oxides and perovskites, *Nucl. Instrum. Methods Phys. Res. Sect. B Beam Interact. Mater. Atoms* 268 (19) (2010) 3084–3089, <https://doi.org/10.1016/j.nimb.2010.05.053>.
- [38] S. Wang, L. Wang, R. Ewing, Electron and ion irradiation of zeolites, *J. Nucl. Mater.* 278 (2–3) (2000) 233–241, [https://doi.org/10.1016/S0022-3115\(99\)00246-9](https://doi.org/10.1016/S0022-3115(99)00246-9).
- [39] F. Orellana-García, M.A. Álvarez, M.V. López-Ramón, J. Rivera-Utrilla, M. Sánchez-Polo, Effect of $\text{HO}\cdot$, textSO_4^- and textCO_3^- radicals on the photodegradation of the herbicide amitrole by UV radiation in aqueous solution, *Chem. Eng. J.* 267 (2015) 182–190, <https://doi.org/10.1016/j.cej.2015.01.019>.
- [40] S. Girard, A. Alessi, N. Richard, L. Martin-Samos, V. De Michele, L. Giacomazzi, S. Agnello, D. Di Francesca, A. Morana, B. Winkler, et al., Overview of radiation induced point defects in silica-based optical fibers, *Rev. Phys.* 4 (2019) 100032, <https://doi.org/10.1016/j.revip.2019.100032>.
- [41] V. Pankratova, A. Kozlova, O. Buzanov, K. Chernenko, R. Shendrik, A. Sarakovskis, V. Pankratov, Time-resolved luminescence and excitation spectroscopy of co-doped $\text{Gd}_3\text{Ga}_3\text{Al}_2\text{O}_{12}$ scintillating crystals, *Sci. Rep.* 10 (2020) 20388, <https://doi.org/10.1038/s41598-020-77451-x>.
- [42] V.Y. Ivanov, E. Shlygin, V. Pustovarov, V. Mazurenko, B. Shul'gin, Intrinsic luminescence of rare-earth oxyorthosilicates, *Phys. Solid State* 50 (9) (2008) 1692–1698, <https://doi.org/10.1134/S1063783408090217>.
- [43] A. Paleari, F. Meinardi, S. Brovelli, R. Lorenzi, Competition between green self-trapped-exciton and red non-bridging-oxygen emissions in SiO_2 under interband excitation, *Commun. Phys.* 1 (1) (2018) 1–12, <https://doi.org/10.1038/s42005-018-0069-5>.
- [44] P. Dorenbos, Modeling the chemical shift of lanthanide 4f electron binding energies, *Phys. Rev. B* 85 (16) (2012) 165107, <https://doi.org/10.1103/PhysRevB.85.165107>.
- [45] R. Shendrik, A. Shalaev, A. Myasnikova, A. Bogdanov, E. Kaneva, A. Rusakov, A. Vasilkovskiy, Optical and structural properties of textEu_2^3+ doped BaBrI and BaClI crystals, *J. Lumin.* 192 (2017) 653–660, <https://doi.org/10.1016/j.jlumin.2017.07.059>.
- [46] E. Kaneva, R. Shendrik, E. Mesto, A. Bogdanov, N. Vlydkin, Spectroscopy and crystal chemical properties of $\text{NaCa}_2[\text{Si}_4\text{O}_{10}]\text{F}$ natural agrellite with tubular structure, *Chem. Phys. Lett.* 738 (2020) 136868, <https://doi.org/10.1016/j.cplett.2019.136868>.
- [47] N. Itoh, T. Eshita, R. Williams, Anticorrelation between yields of recombination luminescence and recombination-induced defect formation in alkali-metal halides, *Phys. Rev. B* 34 (6) (1986) 4230.
- [48] R. Shendrik, A. Myasnikova, A. Rupasov, A. Shalaev, Role of electron and hole centers in energy transfer in BaBrI crystals, *Radiat. Meas.* 122 (2019) 17–21, <https://doi.org/10.1016/j.radmeas.2019.01.008>.
- [49] R. Shendrik, N. Popov, A. Myasnikova, F-centers, In BaBrI single crystal, *IEEE Trans. Nucl. Sci.* 67 (6) (2020) 946–951, <https://doi.org/10.1109/TNS.2020.2983617>.
- [50] A. Shalaev, R. Shendrik, A. Rusakov, A. Bogdanov, V. Pankratov, K. Chernenko, A. Myasnikova, Luminescence of divalent lanthanide doped BaBrI single crystal under synchrotron radiation excitations, *Nucl. Instrum. Methods Phys. Res. Sect. B Beam Interact. Mater. Atoms* 467 (2020) 17–20, <https://doi.org/10.1016/j.nimb.2020.01.023>.
- [51] T.E. Tsai, D.L. Griscom, Experimental evidence for excitonic mechanism of defect generation in high-purity silica, *Phys. Rev. Lett.* 67 (1991) 2517–2520, <https://doi.org/10.1103/PhysRevLett.67.2517>.
- [52] M. Kirm, G. Zimmerer, E. Feldbach, A. Lushchik, C. Lushchik, F. Savikhin, Self-trapping and multiplication of electronic excitations in Al_2O_3 and $\text{Al}_2\text{O}_3:\text{Sc}$, *Phys. Rev. B* 60 (1999) 502–510, <https://doi.org/10.1103/PhysRevB.60.502>.
- [53] A. Lushchik, C. Lushchik, M. Kirm, V. Nagirnyi, F. Savikhin, E. Vasil'chenko, Defect creation caused by the decay of cation excitons and hot electron-hole recombination in wide-gap dielectrics, *Nucl. Instrum. Methods Phys. Res. Sect. B Beam Interact. Mater. Atoms* 250 (1–2) (2006) 330–336.
- [54] V. Natarajan, T. Seshagiri, A. Page, Role of radical ions in the thermally stimulated luminescence of uranium doped BaCO_3 system, *J. Radioanal. Nucl. Chem.* 187 (2) (1994) 123–129.